Année de publication : 2020

C O S Sorzano, F de Isidro-Gómez, E Fernández-Giménez, D Herreros, S Marco, J M Carazo, C Messaoudi (2020 Oct 7)

Improvements on marker-free images alignment for electron tomography.

Journal of structural biology: X : 100037 : DOI : 10.1016/j.yjsbx.2020.100037

Résumé

Electron tomography is a technique to obtain three-dimensional structural information of samples. However, the technique is limited by shifts occurring during acquisition that need to be corrected before the reconstruction process. In 2009, we proposed an approach for post-acquisition alignment of tilt series images. This approach was marker-free, based on patch tracking and integrated in free software. Here, we present improvements to the method to make it more reliable, stable and accurate. In addition, we modified the image formation model underlying the alignment procedure to include different deformations occurring during acquisition. We propose a new way to correct these computed deformations to obtain reconstructions with reduced artifacts. The new approach has demonstrated to improve the quality of the final 3D reconstruction, giving access to better defined structures for different transmission electron tomography methods: resin embedded STEM-tomography and cryo-TEM tomography. The method is freely available in TomoJ software.

Adrià Sogues, Mariano Martinez, Quentin Gaday, Mathilde Ben Assaya, Martin Graña, Alexis Voegele, Michael VanNieuwenhze, Patrick England, Ahmed Haouz, Alexandre Chenal, Sylvain Trépout, Rosario Duran, Anne Marie Wehenkel, Pedro M Alzari (2020 Apr 4)

Essential dynamic interdependence of FtsZ and SepF for Z-ring and septum formation in Corynebacterium glutamicum.

Nature communications : 1641 : DOI : 10.1038/s41467-020-15490-8

Résumé

The mechanisms of Z-ring assembly and regulation in bacteria are poorly understood, particularly in non-model organisms. Actinobacteria, a large bacterial phylum that includes the pathogen Mycobacterium tuberculosis, lack the canonical FtsZ-membrane anchors and Z-ring regulators described for E. coli. Here we investigate the physiological function of Corynebacterium glutamicum SepF, the only cell division-associated protein from Actinobacteria known to interact with the conserved C-terminal tail of FtsZ. We show an essential interdependence of FtsZ and SepF for formation of a functional Z-ring in C. glutamicum. The crystal structure of the SepF-FtsZ complex reveals a hydrophobic FtsZ-binding pocket, which defines the SepF homodimer as the functional unit, and suggests a reversible oligomerization interface. FtsZ filaments and lipid membranes have opposing effects on SepF polymerization, indicating that SepF has multiple roles at the cell division site, involving FtsZ bundling, Z-ring tethering and membrane reshaping activities that are needed for proper Z-ring assembly and function.

Emilie Mathieu, Anne-Sophie Bernard, H Y Vincent Ching, Andrea Somogyi, Kadda Medjoubi, Jennifer Rodon Fores, Hélène C Bertrand, Amandine Vincent, Sylvain Trépout, Jean-Luc Guerquin-Kern, Andreas Scheitler, Ivana Ivanović-Burmazović, Philippe Seksik, Nicolas Delsuc, Clotilde Policar (2020 Feb 6)

Anti-inflammatory activity of superoxide dismutase mimics functionalized with cell-penetrating peptides.

Dalton transactions (Cambridge, England : 2003) : 49 : 2323-2330 : DOI : 10.1039/c9dt04619d

Résumé

A superoxide dismutase mimic (Mn1) was functionalized with three positively charged-peptides: RRRRRRRRR (Mn1-R9), RRWWWRRWRR (Mn1-RW9) or F-r-F-K (Mn1-MPP). Characterization of the physico-chemical properties of the complexes show that they share similar binding affinity for Mn, apparent reduction potential and intrinsic superoxide dismutase activity. However, their accumulation in cells is different (Mn1-R9 < Mn1-MPP < Mn1-RW9 < Mn1), as well as their subcellular distribution. In addition, the three functionalized-complexes display a better anti-inflammatory activity than Mn1 when assayed at 10 µM. This improvement is due to a combination of an anti-inflammatory effect of the peptidyl moiety itself, and of the SOD mimic for Mn1-RW9 and Mn1-MPP. In contrast, the enhanced anti-inflammatory activity of Mn1-R9 is solely due to the SOD mimic.

Année de publication : 2019

Tao X., Chen H., Trepout S., Cen J., Ling J., Li M.H. (2019 Oct 15)

Polymersomes with Aggregation-Induced Emission Based on Amphiphilic Block Copolypeptoids

Chem. Commun. : 55 : -13530-13533 : DOI : 10.1039/C9CC07501A

Résumé

Biocompatible polymersomes are prepared from amphiphilic block copolypeptoids with aggregation-induced emission, where the hydrophobic block P(TPE-NAG) is a tetraphenylethylene (TPE)-modified poly(N-allylglycine) and the hydrophilic block is polysarcosine. These nanoparticles are non-cytotoxic and show strong fluorescence emission in aqueous solution.

Yangwei Deng, Hui Chen, Xinfeng Tao, Fangyi Cao, Sylvain Trépout, Jun Ling, Min-Hui Li (2019 Jul 31)

Oxidation-Sensitive Polymersomes Based on Amphiphilic Diblock Copolypeptoids.

Biomacromolecules : 20 : 3435-3444 : DOI : 10.1021/acs.biomac.9b00713

Résumé

Stimuli-responsive polymersomes formed by amphiphilic block copolymers have attracted substantial attention as smart and robust containers for drug delivery and nano/microreactors. Biosourced amphiphilic diblock copolypeptoids were developed that can self-assemble into oxidation-responsive unilamellar vesicles. These vesicles can burst under the action of reactive oxygen species which can be the hydrogen peroxide or the singlet oxygen produced by light-activation of a photosensitizer with spatiotemporal control. Polysarcosine (PSar, also called poly(-methyl glycine)) was selected as the hydrophilic block because of its resistance to protein adsorption and low toxicity, similar to poly(ethylene glycol) (PEG). We designed and synthesized poly(-3-(methylthio)propyl glycine) as the hydrophobic block. Its polyglycine backbone is the same as that of PSar, and especially, its hydrophobic N-substituents, thioether side chains, can be oxidized to hydrophilic sulfoxides. These oxidation-responsive polymersomes entirely based on N-substituted poly(amino acid)s were biocompatible as confirmed by cell viability tests and may find applications in drug delivery, biosensing, biodetection, and nano/microreactors.

Sylvain Trépout (2019 Jul 19)
Tomographic Collection of Block-Based Sparse STEM Images: Practical Implementation and Impact on the Quality of the 3D Reconstructed Volume.
Materials (Basel, Switzerland) : DOI : E2281

Résumé

The reduction of the electron dose in electron tomography of biological samples is of high significance to diminish radiation damages. Simulations have shown that sparse data collection can perform efficient electron dose reduction. Frameworks based on compressive-sensing or inpainting algorithms have been proposed to accurately reconstruct missing information in sparse data. The present work proposes a practical implementation to perform tomographic collection of block-based sparse images in scanning transmission electron microscopy. The method has been applied on sections of chemically-fixed and resin-embedded cells. There are 3D reconstructions obtained from various amounts of downsampling, which are compared and eventually the limits of electron dose reduction using this method are explored.

David Partouche, Jérémie Mathurin, Antoine Malabirade, Sergio Marco, Christophe Sandt, Véronique Arluison, Ariane Deniset-Besseau, Sylvain Trépout (2019 Apr 1)
Correlative infrared nanospectroscopy and transmission electron microscopy to investigate nanometric amyloid fibrils: prospects and challenges.
Journal of microscopy : 274 : 23-31 : DOI : 10.1111/jmi.12779

Résumé

Propagation of structural information through conformational changes in host-encoded

amyloid proteins is at the root of many neurodegenerative disorders. Although important breakthroughs have been made in the field, fundamental issues like the 3D-structures of the fibrils involved in some of those disorders are still to be elucidated. To better characterise those nanometric fibrils, a broad range of techniques is currently available. Nevertheless none of them is able to perform direct chemical characterisation of single protein fibrils. In this work, we propose to investigate the structure of the C-terminal region of a bacterial protein called Hfq as a model amyloidogenic protein, using a correlative approach. The complementary techniques used are transmission electron microscopy and a newly developed infrared nanospectroscopy technique called AFM-IR. We introduce and discuss the strategy that we have implemented as well as the protocol, challenges and difficulties encountered during this study to characterise amyloid assemblies at the nearly single-molecule level. LAY DESCRIPTION: Propagation of structural information through conformational changes in amyloid proteins is at the root of many neurodegenerative disorders. Amyloids are nanostructures originating from the aggregation of multiple copies of peptide or protein monomers that eventually form fibrils. Often described as being the cause for the development of various diseases, amyloid fibrils are of major significance in the public health domain. While important breakthroughs have been made in the field, fundamental issues like the 3D-structures of the fibrils implied in some of those disorders are still to be elucidated. To better characterise these fibrils, a broad range of techniques is currently available for the detection and visualisation of amyloid nanostructures. Nevertheless none of them is able to perform direct chemical characterisation of single protein fibrils. In this work, we propose to investigate the structure of model amyloidogenic fibrils using a correlative approach. The complementary techniques used are transmission electron microscopy and a newly developed infrared nanospectroscopy technique called AFM-IR that allows chemical characterisation at the nanometric scale. The strategy, protocol, challenges and difficulties encountered in this approach are introduced and discussed herein.

Année de publication : 2018

Tom Baladi, Jessy Aziz, Florent Dufour, Valentina Abet, Véronique Stoven, François Radvanyi, Florent Poyer, Ting-Di Wu, Jean-Luc Guerquin-Kern, Isabelle Bernard-Pierrot, Sergio Marco Garrido, Sandrine Piguel (2018 Nov 1)

Design, synthesis, biological evaluation and cellular imaging of imidazo[4,5-b]pyridine derivatives as potent and selective TAM inhibitors.

Bioorganic & medicinal chemistry : 26 : 5510-5530 : DOI : 10.1016/j.bmc.2018.09.031

Résumé

The TAM kinase family arises as a new effective and attractive therapeutic target for cancer therapy, autoimmune and viral diseases. A series of 2,6-disubstituted imidazo[4,5-b]pyridines were designed, synthesized and identified as highly potent TAM inhibitors. Despite remarkable structural similarities within the TAM family, compounds 28 and 25 demonstrated high activity and selectivity in vitro against AXL and MER, with IC value of 0.77 nM and 9 nM respectively and a 120- to 900-fold selectivity. We also observed an unexpected nuclear localization for compound 10Bb, thanks to nanoSIMS technology, which could be correlated to the absence of cytotoxicity on three different cancer cell lines being

sensitive to TAM inhibition.

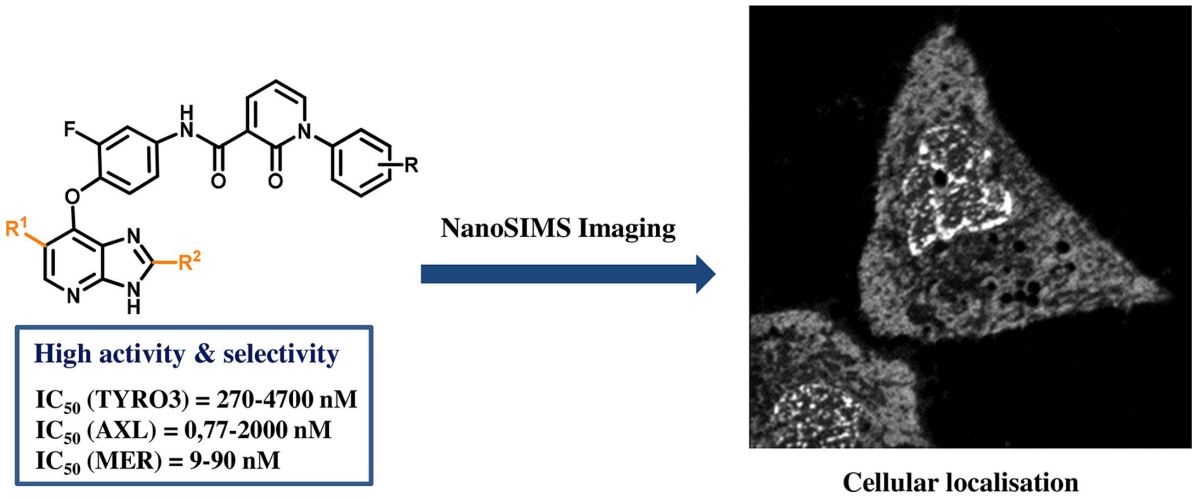

Marlène Rasschaert, Josef A Schroeder, Ting-Di Wu, Sergio Marco, Andréa Emerit, Heiko Siegmund, Claudia Fischer, Nathalie Fretellier, Jean-Marc Idée, Claire Corot, Christoph Brochhausen, Jean-Luc Guerquin-Kern (2018 Jul 10)

Multimodal Imaging Study of Gadolinium Presence in Rat Cerebellum: Differences Between Gd Chelates, Presence in the Virchow-Robin Space, Association With Lipofuscin, and Hypotheses About Distribution Pathway.

Investigative radiology : 53 : 518-528 : DOI : 10.1097/RLI.0000000000000490

Résumé

Purpose The aim of this study was to investigate, based on in-depth multimodal imaging, the presence of Gd deposits, their ultrastructure, location, and co-location with endogenous elements, in the cerebellum, after repeated administrations of gadolinium-based contrast agents (GBCAs).

Methods Rats sensitized by subtotal nephrectomy received 20 daily intravenous injections of 0.6 mmol Gd/kg for 5 weeks of commercial forms of either gadoterate, gadobenate or gadodiamide, or saline (n = 2/group). The study was randomized and blinded. Magnetic resonance imaging examination was performed weekly. One month after the last injection, electron microscopy analysis of the deep cerebellar nuclei, the granular layer of cerebellar cortex, and the choroid plexus was performed. Elemental analysis of deposits was carried out by electron energy loss spectroscopy. Secondary ion mass spectroscopy was used for complementary chemical mapping.

Results A T1 hypersignal was evidenced in the deep cerebellar nuclei of rats treated with linear GBCAs, and Gd deposits were identified in all the studied cerebellar structures with gadobenate and gadodiamide (except in the granular layer in gadobenate-treated rats). No such effect was found with the macrocyclic GBCA gadoterate. Most of the Gd deposits

revealed a characteristic spheroid "sea urchin-like" morphology, rich in phosphorus, and were localized in the basal lamina of microvessels, in the perivascular Virchow-Robin space, and in the interstitium. Gd was also identified in the glial cells, associated with lipofuscin pigments, for these same groups.

Conclusions Transmission electron microscopy analysis of cerebellums of renally impaired rats repeatedly injected with gadobenate and gadodiamide revealed the presence of Gd. Spheroid Gd depositions consisting of a filamentous meshwork were observed in the wall of microvessels, in perivascular Virchow-Robin space, and in the interstitium. Gd was also found in choroid plexus and was associated with pigments (likely lipofuscin) in glial cells. This is consistent with the involvement of the glymphatic distribution pathway for GBCAs. No insoluble Gd deposits were detected in rats injected with the macrocyclic GBCA gadoterate and controls.

Ptissam Bergam, Johannes M Reisecker, Zsófia Rakvács, Nóra Kucsma, Graça Raposo, Gergely Szakacs, Guillaume van Niel (2018 Jun 26)

ABCB6 Resides in Melanosomes and Regulates Early Steps of Melanogenesis Required for PMEL Amyloid Matrix Formation.

Journal of molecular biology : 3802-3818 : DOI : S0022-2836(18)30662-4

Résumé

Genetically inheritable pigmentation defects provide a unique opportunity to reveal the function of proteins contributing to melanogenesis. Dyschromatosis universalis hereditaria (DUH) is a rare pigmentary genodermatosis associated with mutations in the ABCB6 gene. Here we use optical and electron microscopy imaging combined with biochemical tools to investigate the localization and function of ABCB6 in pigment cells. We show that ABCB6 localizes to the membrane of early melanosomes and lysosomes of the human melanocytic cell line MNT-1. Depletion of ABCB6 by siRNA impaired PMEL amyloidogenesis in early melanosomes and induced aberrant accumulation of multilamellar aggregates in pigmented melanosomes. PMEL fibril formation and normal maturation of pigmented melanosomes could be restored by the overexpression of wild-type ABCB6 but not by variants containing an inactivating catalytic mutation (K629M) or the G579E DUH mutation. In line with the impairment of PMEL matrix formation in the absence of ABCB6, morphological analysis of the retinal pigment epithelium of ABCB6 knockout mice revealed a significant decrease of melanosome numbers. Our study extends the localization of ABCB6 to melanosomes, suggesting a potential link between the function of ABCB6 and the etiology of DUH to amyloid formation in pigment cells.

Ana Vujic, Carolin Lerchenmüller, Ting-Di Wu, Christelle Guillermier, Charles P Rabolli, Emilia Gonzalez, Samuel E Senyo, Xiaojun Liu, Jean-Luc Guerquin-Kern, Matthew L Steinhauser, Richard T Lee, Anthony Rosenzweig (2018 Apr 27)

Exercise induces new cardiomyocyte generation in the adult mammalian heart.
Nature communications : 9 : 1659 : DOI : 10.1038/s41467-018-04083-1

Résumé

Loss of cardiomyocytes is a major cause of heart failure, and while the adult heart has a limited capacity for cardiomyogenesis, little is known about what regulates this ability or whether it can be effectively harnessed. Here we show that 8 weeks of running exercise increase birth of new cardiomyocytes in adult mice (~4.6-fold). New cardiomyocytes are identified based on incorporation of N-thymidine by multi-isotope imaging mass spectrometry (MIMS) and on being mononucleate/diploid. Furthermore, we demonstrate that exercise after myocardial infarction induces a robust cardiomyogenic response in an extended border zone of the infarcted area. Inhibition of miR-222, a microRNA increased by exercise in both animal models and humans, completely blocks the cardiomyogenic exercise response. These findings demonstrate that cardiomyogenesis can be activated by exercise in the normal and injured adult mouse heart and suggest that stimulation of endogenous cardiomyocyte generation could contribute to the benefits of exercise.

Année de publication : 2017

Sylvain Trépout, Anne-Marie Tassin, Sergio Marco, Philippe Bastin (2017 Dec 18)
STEM tomography analysis of the trypanosome transition zone.
Journal of structural biology : 51-60 : DOI : S1047-8477(17)30228-9

Résumé

The protist Trypanosoma brucei is an emerging model for the study of cilia and flagella. Here, we used scanning transmission electron microscopy (STEM) tomography to describe the structure of the trypanosome transition zone (TZ). At the base of the TZ, nine transition fibres irradiate from the B microtubule of each doublet towards the membrane. The TZ adopts a 9 + 0 structure throughout its length of ~300 nm and its lumen contains an electron-dense structure. The proximal portion of the TZ has an invariant length of 150 nm and is characterised by a collarette surrounding the membrane and the presence of electron-dense material between the membrane and the doublets. The distal portion exhibits more length variation (from 55 to 235 nm) and contains typical Y-links. STEM analysis revealed a more complex organisation of the Y-links compared to what was reported by conventional transmission electron microscopy. Observation of the very early phase of flagellum assembly demonstrated that the proximal portion and the collarette are assembled early during construction. The presence of the flagella connector that maintains the tip of the new flagellum to the side of the old was confirmed and additional filamentous structures making contact with the membrane of the flagellar pocket were also detected. The structure and potential functions of the TZ in trypanosomes are discussed, as well as its mode of assembly.

Slodzian G., Wu T.D., Duprat J., Engrand C., Guerquin-Kern J.L. (2017 Dec 1)

Dynamic transfer applied to secondary ion imaging over large scanned fields with the nanoSIMS 50 at high mass resolution

Nuclear Instruments and Methods in Physics Research Section B: Beam Interactions with Materials and Atoms : 412 : 123-173 : DOI : 10.1016/j.nimb.2017.06.019

Résumé

Dynamic transfer is an adaptive optical approach used for coupling a scanning ion probe with the mass spectrometer designed for analyzing sputtered ions emanating from the probe impact. Its tuning is of crucial importance for getting uniform signal collection over large scanning fields and therefore scanning images free of vignetting in a context of high mass resolution. Revisiting the optical design of the NanoSIMS 50 instrument, where the same set of lenses focuses the primary ion probe on the sample and collects secondary ions from the sample, led us to develop novel experimental procedures to achieve dynamic transfer tuning and overcome instrumental imperfections. It is the case for scanning distortion that may be induced by the octopole used for correcting probe astigmatism and may cause irreducible vignetting on scanning images. We show that it is possible to develop complete tuning procedures by compromising temporarily on the sharpness of the probe focus. Most importantly, we show that, in a context of high mass resolution, the transfer does not significantly disturb isotopic ratios over large scanned fields provided external coils are properly adjusted to compensate ambient magnetic fields.

Deepening the procedures led us to demonstrate that the scanning center of the probe may not coincide with the imaging center of COOL, Coaxial Objective Lenses forming the probe and extracting secondary ions. We have checked that bringing those two centers into coincidence resulted in a better image quality over large fields.

In the present work, we show how to handle the secondary beam in order to position it before it enters the spectrometer. That capability is essential for optimizing transmission at high mass resolution by aligning the secondary beam axis on a given entrance axis of the spectrometer.

These results led us to propose several instrumental improvements including the crucial interest of an additional octopole upstream in the primary ion probe column to prevent scanning distortion when performing astigmatism correction and the possibility of offsetting primary beam deviating plates to bring scanning and imaging centers in coincidence.

Sylvain Trépout, Anne Marie Wehenkel (2017 Sep 5)

Bacterial Tubulins: A Eukaryotic-Like Microtubule Cytoskeleton.

Trends in microbiology : 782-784 : DOI : S0966-842X(17)30194-4

Résumé

Ever since their discovery, bacterial tubulins, found in several Prosthecobacter species, have raised curiosity as they are closely related to eukaryotic tubulin. Deng and colleagues now

present new evidence for the functional homology of the two cytoskeletal systems where in vitro reconstituted Btub-microtubules display eukaryote-like biochemical and dynamic properties.

Ilse Hurbain, Maryse Romao, Ptissam Bergam, Xavier Heiligenstein, Graça Raposo (2017 May 1)
Analyzing Lysosome-Related Organelles by Electron Microscopy.
Methods in molecular biology (Clifton, N.J.) : 43-71 : DOI : 10.1007/978-1-4939-6934-0_4

Résumé

Intracellular organelles have a particular morphological signature that can only be appreciated by ultrastructural analysis at the electron microscopy level. Optical imaging and associated methodologies allow to explore organelle localization and their dynamics at the cellular level. Deciphering the biogenesis and functions of lysosomes and lysosome-related organelles (LROs) and their dysfunctions requires their visualization and detailed characterization at high resolution by electron microscopy. Here, we provide detailed protocols for studying LROs by transmission electron microscopy. While conventional electron microscopy and its recent improvements is the method of choice to investigate organelle morphology, immunoelectron microscopy allows to localize organelle components and description of their molecular make up qualitatively and quantitatively.